Published in final edited form as:
J Neurosci Methods. 2008 August 30; 173(2): 279–285. doi:10.1016/j.jneumeth.2008.06.024.

Characterization of flexible ECoG electrode arrays for chronic recording in awake rats

John D. Yeager[a], **Derrick J. Phillips**[b], **David M. Rector**[b], and **David F. Bahr**[a]

a*School of Mechanical and Materials Engineering, Washington State University, Pullman, WA 99164, USA*

b*Department of Veterinary Comparative Anatomy Physiology and Pharmacology, Washington State University, Pullman, WA 99164, USA*

Abstract

We developed a 64 channel flexible polyimide ECoG electrode array and characterized its performance for long term implantation, chronic cortical recording and high resolution mapping of surface evoked potentials in awake rats. To achieve the longest possible recording periods, the flexibility of the electrode array, adhesion between the metals and carrier substrate, and biocompatibility was critical for maintaining the signal integrity. Experimental testing of thin film adhesion was applied to a gold – polyimide system in order to characterize relative interfacial fracture energies for several different adhesion layers, yielding an increase in overall device reliability. We tested several different adhesion techniques including: gold alone without an adhesion layer, titanium-tungsten, tantalum and chromium. We found the titanium-tungsten to be a suitable adhesion layer considering the biocompatibility requirements as well as stability and delamination resistance. While chromium and tantalum produced stronger gold adhesion, concerns over biocompatibility of these materials require further testing. We implanted the polyimide ECoG electrode arrays through a slit made in the skull of rats and recorded cortical surface evoked responses. The arrays performed reliably over a period of at least 100 days and signals compared well with traditional screw electrodes, with better high frequency response characteristics. Since the ultimate goal of chronically implanted electrode arrays is for neural prosthetic devices that need to last many decades, other adhesion layers that would prove safe for implantation may be tested in the same way in order to improve the device reliability.

Keywords

Surface Evoked Potential; Polyimide; Kapton; Biocompatibility; Device Durability

1. Introduction

1.1 Neurological recording techniques

Recording evoked responses from the cortical surface using electrocoticogram (ECoG) surface electrode arrays can provide detailed mapping of cortical surface activation without penetrating the tissue (Jones and Barth, 1999). Insight into the duration, response time and intensity of

Corresponding Author: David M. Rector, PhD., Dept. VCAPP, Washington State University, 205 Wegner Hall, Pullman, WA 99164, Ph: 509-335-1587 Fax: 509-335-4650, Email: drector@wsu.edu.

these signals may shed light on the mechanisms by which the brain interprets external stimuli (Prigg et al., 2002). Several different techniques exist for recording brain signals in rats, depending on the type of measurement desired. In many animal protocols, traditional screw electrodes are placed over the skull to record EEG and evoked responses from large cortical regions. Because of their size, the spatial resolution of screw electrodes is poor. Similarly, human EEG scalp recordings are low resolution due to current spread through the dura, skull and skin. In the human neurosurgery, subdural ECoG electrodes record obtain signals directly from the cortical surface, with higher spatial resolution allowing 30 or more locations to be simultaneously probed (Penfield and Boldrey, 1937). By using microfabrication and photolithography techniques, ECoG electrode arrays can be much higher resolution than typical human arrays, and map individual cortical columns (Hollenberg et al., 2006).

Since the ECoG arrays are closer to the cortical surface than screw electrodes, the lower capacitance allows them to record high frequency components with better fidelity. In rats, neural firing in cortex directly correlates with external stimulation (Woolsey and Van der Loos, 1970). Thus, when using high quality amplifiers with low noise and high bandwidth characteristics, several investigators have observed signals from cortical ECoG arrays that correlate directly to population action potentials and excitatory post synaptic potentials, potentially reducing the need for penetrating electrodes in cortical recording (Jones et al., 2000). To obtain local field potentials or multi-unit action potentials, direct implantation of microwires in mammals has proven exceptionally useful (Strumwasser, 1958). However, for chronic studies, the tissue response to penetrating wire electrodes can lead to experimental difficulties from mechanical trauma (Schmidt et al., 1993), long term inflammation (Szarowski et al., 2003), and the glial scar formation (Maynard et al., 2000). A comprehensive review on penetrating electrode implantation issues is given by Polikov et al (2005). Thus, for long term prosthetic devices, electrodes that do not penetrate the neural tissue would be desirable. In addition to brain tissue responses, simply implanting any type of electrode array may necessitate the removal of large skull areas (Jones and Barth, 1999; Bjornsson et al., 2006). Thin, flexible electrode arrays can be inserted through a small slit in the skull and record cortical signals while creating electrical maps of the surface, removing the need to penetrate tissue as well as reducing overall trauma of large skull openings (Hollenberg et al., 2006; Cheung et al., 2007).

We have previously developed implantable flexible electrode arrays for cortical recording using biocompatible materials (Hollenberg et al., 2006). For ease of use, we chose Kapton™ (DuPont Chemical Corp, Wilmington, DE), a polyimide with high thermal stability. Polyimides have been used successfully in flexible biomedical implants, showing no reactivity with tissue or bodily fluid (Stieglitz and Meyer, 1999). Some polyimides have shown relatively large water absorption, swelling by 2% (Hetke et al., 1990), causing metal-polymer interface strain. Sodium cations can diffuse preferentially into and along the metal-polymer interface, potentially resulting in blister formation and film delamination (Pommersheim et al., 1995; Leng et al., 1999). For a sufficiently weak interface, the implantation strain and processing may cause delamination regardless of ion accumulation. However, some polyimides with lower water uptake, around 0.5%, have been successfully used for implantable electrodes (Steiglitz et al., 2002).

In our eariler study, gold was used as the conductive substrate, and an SU-8 polymer coating was utilized to isolate the gold electrodes as well as to protect them from external damage (Hollenberg et al., 2006). These arrays were successful for a short-term study of acute rats, but array durability may be a concern for chronic long-term implantation. Specifically, experiments on the electrode system indicated that the gold might delaminate from the Kapton at approximately 1% strain; a level that might occur during implantation. Additionally, no consideration of the electrode long-term durability*in vivo* was made in this previous study.

To ensure device longevity for chronic implantation, we assessed the durability of the gold-polyimide interface. Several methods of improving noble metal adhesion, such as gold, to polymeric materials have been investigated. Plasma etching of the polyimide surface may increase the surface energy through imide ring opening, creating additional C-O and C-OH bonds resulting in increased metal adhesion to the surface (Nakamura et al., 1996). Short oxygen plasma etching periods prove effective for increasing the interfacial energy and therefore the gold adhesion to Kapton (Yeager et al., 2007). Other processing paramaters could theoretically be altered to improve adhesion, such as reductions in residual stress due to film thickness and microstructure (Lawrence et al., 2003). However, the film thickness in these electrodes is largely restricted by the requirement of minimal trauma upon implantation. Another option, explored in this current study, is to include a metal adhesion layer between the gold and Kapton.

We considered three metal adhesion layers: chromium, tantalum, and a titanium-tungsten alloy. Under certain conditions, chromium may be a suitable adhesion layer for implantable electrodes (Mailley et al., 2004; Soden et al., 2004), and some chromium alloys may be nontoxic (Merrill et al., 2005), but these results require further testing. Tantalum has also been used to improve gold adhesion to various substrates, but yields somewhat poorer results than chromium (Haq et al., 1969). Additionally, tantalum may be biocompatible for prosthetics but is considered “reactive” for neural implantation (Matsuno et al., 2000; Merrill et al., 2005). Both titanium and tungsten are considered biocompatible and non-reactive and have been used in neural interfaces as an adhesion layer for gold (Kim et al., 2007; Jalonen and Tuominen, 2002).

1.2 4-point bend testing

Small-scale four point bend testing is a useful method of isolating delamination energy and quantifying film adhesion to a substrate through a linear elastic fracture mechanics (LEFM) based approach (Dauskardt et al., 1998). Figure 1A schematically shows a typical four point testing arrangement for thin film adhesion testing. The testing geometry consists of two elastic layers (silicon or glass are common choices) that sandwich a set of film systems. The top of the composite beam is notched with a diamond scribe to initiate a crack site. The load is applied and displacement is measured as the crack propagates. The crack moves vertically through the top layer until it reaches the interfacial layer. The crack then may continue its vertical descent or it may propagate laterally. The strength of adhesion between the film and the substrate controls the crack direction, as the crack will travel along the path of least resistance (Daukardt et al., 1998).

If the crack propagates laterally along a specimen interface, the load-displacement curve shows a distinctive plateau (Dauskardt et al., 1998), which can depend on the testing conditions (Hughey et al., 2004). The load at this plateau can then be used in Eq. 1 to find the strain energy release rate, G, which characterizes the toughness of the interface. In the purely elastic case, the energy release rate (per unit area) at delamination is given by

$$G=g\frac{L^2P^2(1-\nu^2)}{EB^2H^3} \qquad \text{(Eq. 1)}$$

where L is distance between an inner and outer pin, P is the applied load at the plateau, ν is Poisson’s ratio, E is the modulus of the elastic substrate, and B and H are respectively the width and height of the specimen, as shown in Figure 1A. The geometric factor, g, depends on the elastic substrate thickness and is 0.13125 for our study (Huang et al., 2005). The energy release rate is equal to the crack extension energy per unit area during crack propagation.

The mechanics for the bend tests are suitable for perfectly elastic systems, since plastic deformation and other non-elastic processes may affect the measurement. However, by

utilizing a consistent thicknesses of Kapton to a brittle elastic, material should yield relative, if not absolute, quantitative information about the interfacial toughness of the system. Additionally, using elastic plates constrains and minimizes subsequent plasticity in the interface. We characterized the adhesion characteristics for several substrates, and tested the titanium-tungsten technique in animals chronically implanted with the array to assess the signal quality over time.

2. Material and Methods

2.1 Electrode fabrication

Electrode arrays were fabricated in a Class 1000 clean room to minimize contamination. The polyimide film (Kapton, DuPont Chemical Corp,Wilmington, DE) was purchased in 25μ m thick rolls, and secured to a glass slide for subsequent processing. After a preliminary cleaning process, the Kapton was O_2 plasma etched at 100W for three minutes. The etching was done to chemically alter the surface of the polyimide in order to enhance adhesion (Yeager et al., 2007; Supriya and Claus, 2004). Immediately after etching the Kapton was transferred to a DC Magnetron sputtering system with two metallic targets, which was evacuated to a base pressure of less than 1×10^{-6} torr. Gold was sputter deposited to a thickness of 300 nm. In the cases where an adhesion layer was utilized, 5nm of the metal layer was sputtered directly before the gold. In all cases, vacuum was not broken between the metal film deposition.

After sputtering, the specimens were spin-coated with a photoresist for photolithographic patterning. A positive photomask pattern (chrome patterned on glass) was placed over the specimen and the whole assembly was exposed to UV light for 45 seconds. The UV radiation chemically altered the exposed portions of the photoresist, resulting in regions susceptible to removal by a developing solution. After development, the specimen had both regions of exposed gold and of gold covered with the patterned photoresist. The exposed gold was then removed with an iodine based chemical etch (TFA, Transene Company Inc., Danvers, MA), at room temperature through a liquid immersion process, leaving only gold in the desired pattern. After patterning, a thick photoresist (SU-8, Shipley Manufacturing, Marlborough, MA) was spin-coated to a thickness of approximately 10 μ m. This thickness provides a slight stress in the film that balances any stresses that are present in the gold layer, allowing for a finished film that is effectively flat. A similar photolithographic procedure was used to pattern the protective polymeric layer over the gold, allowing for precise areas of the gold electrode to be exposed. Specifically, only the dot array for brain contact and the electrode pads for electronic signal measurement were exposed. After another cleaning process, the electrodes were ready for implantation. For a more detailed procedure, refer to Hollenberg et al. (2006).

2.2 Electrode implantation

We chronically implanted an electrode array on the surface of the cortex in three female Sprague-Dawley rats. All surgical procedures were performed in accordance with the “Guide for the Care and Use of Laboratory Animals” approved by the Washington State University Animal Care and Use Committee. Isoflurane (5.0%) was used to induce anesthesia followed by maintenance of anesthesia (1.0–2.0%) in oxygen. Toe pinch reflex, heart rate, and respiration were used to track the depth of anesthesia. A 5×1 mm area of bone was removed 1mm medial to the temporal ridge and 1 mm rostral to lambda, and the 5×5 mm gold on Kapton electrode array was inserted between the bone and the dura over the auditory and somatosensory cortex. A stainless steel screw electrode was placed over the frontal lobe to determine animal behavioral state, and another over the parietal lobe next to the gold electrodes as a control screw electrode (Fig. 2). Two screws placed over the occipital lobe served as a ground reference. One dose of penicillin (0.1 mL IM each leg, total dose = 10,000 iu/kg) was given at the end of the surgery. Flunixin (1.1 mg/kg Sbc.) was given as a pain reliever and anti-inflammatory agent

for 3 days after the surgery. Two weeks of surgical recovery elapsed before recording commenced.

One week after recovery from surgery, animals were connected to our amplifier system and tethered through a thin cable and commutator which allowed free movement with in a 30×30×50cm box. We stimulated the auditory cortex using speaker clicks (200μs pulse) at random intervals of 1–2s for 30 minutes. The electrical signals from the electrodes were filtered between 0.1 Hz and 3.2kHz, then sampled at 20 kHz using a custom data system (Rector and George, 2001). We recorded about 1000 evoked response potentials (ERP) per session and the average ERP amplitude was calculated for each gold ECoG electrode and skull screw electrode.

2.3 Bend test specimen preparation

For all four point bend tests, specimens were prepared up to the point of patterning and etching. Two samples were then bonded to silicon substrates with Epon 440 epoxy (3M, St. Paul, MN) and also to each other, as illustrated in Figure 1B. One side of the four point specimen was notched with a diamond-tipped scribe. The crack path shown in Figure 1B assumed that the crack preferentially propagated through the polyimide rather than delaminating it from the silicon. In order to ensure propagation through the Kapton film, a razor was used to score the Kapton film prior to specimen fabrication. The notch on the Kapton was aligned with the notch in the silicon during fabrication. This greatly decreased the energy required for the crack to pass through the film, and thus the weakest interface was the metal-polymer boundary. Figure 1B is a cross-sectional view of the four point bend specimen and shows the crack path to the interface of interest. The figure is not to scale; the thin layers are enlarged in order to show detail.

3. Results

We tested three different electrode interfacial adhesion layers using the four point bend test illustrated in Figure 1A: a titanium-tungsten alloy (10%Ti-90%W by weight), pure tantalum (Ta), and pure chromium (Cr). Figure 3 shows typical load-displacement curves from the four point bend tests for each interlayer material. Due to the complex nature of the specimens, it was necessary to ensure that the calculated interfacial energy was for the correct interface. Several interfacial crack paths were possible: between the metal and polyimide, between the polyimide and silicon, or between the metal and epoxy. A combination of optical microscopy and X-ray photoelectron spectroscopy (XPS) was used to determine the delaminating interface. Optical inspection of a typical fracture surface revealed exposed Kapton without the gold coating, indicating that gold-polyimide delamination occurred during the test.

While visual inspection suggested metal-polyimide delamination, it was not possible, using optical microscopy, to definitively state whether the delamination was between the adhesion layer and the Kapton or between the adhesion layer and the gold. Therefore XPS, using a AXIS-165 model (Kratos Analytical, Inc., Chestnut Ridge, NY), was performed on the fracture surface, and the resulting spectra for a sample with a Ti-W adhesion layer is shown in Figure 4. The binding energy was calibrated against gold (Au) 4f 7/2 to be 84 eV and highly ordered pyrolytic graphite (HOPG) carbon (C), 1s at 284.5 eV. Peaks in the spectra were identified in Figure 4. Small peaks of Ti and Au and a large tungsten (W) peak on the “epoxy side” indicate that the Ti-W layer peeled away from the Kapton, unambiguously showing that the fracture occurred at the Ti-W-Kapton interface. This was a positive result, showing that the limiting factor to electrode reliability was indeed the delamination resistance of the adhesion layer rather than the gold (i.e. the gold was well adhered to the adhesion layer).

Bend tests were carried out on four sets of specimens: Au only, Au with Ti-W, Au with Ta, and Au with Cr. The Kapton layer in each specimen had been plasma etched as described in

the methods section. Using the load plateaus from the load-displacement curves (as illustrated in Fig. 3) and recording the specimen geometric dimensions, Equation 1 was used to calculate the interfacial adhesion energy for each system (Fig. 5).

Several Ti-W-Au-Kapton ECoGelectrodes were fabricated and implanted in rats for a period of up to 100 days. Figure 6 shows typical ECoG and screw electrode channels responding to neural signals at several intervals post-implantation. The ERP amplitude recorded from the ECoG gold electrode was similar in shape (Fig. 6) and size to the ERP recorded from the screw electrode (Fig. 7). Due to difficulty in presenting the same stimulus intensity between recording days, the ERP amplitude was not constant across days (Fig. 7, bottom panel). Plotting the ECoG electrode amplitude against the screw electrode amplitude for each recording day shows a good relationship between the two signals (Fig. 7, middle and top panels), though the screw electrode exhibited higher variability and higher amplitude than the ECoG electrode (ECoG/screw r=0.9), perhaps due to the larger surface area sampled by the screw electrode. Additionally, the ECoG signals contained significantly higher power in the high frequency components from 100 to 5000 Hz than the screw electrode (Fig. 8) while the screw electrode contained more power in the 20 to 100 Hz range.

4. Discussion

Our measurements indicate that Cr provides the best adhesion layer for these flexible electrodes of the three systems tested in this study. However, for neural implantation the biocompatibility or toxicity of the metals must also be considered. Ti-W was chosen as a suitable adhesion layer for use in our initial long term implantation for its combination of durability and biocompatibility. Other non-toxic adhesion layers are currently being tested in an effort to make the best flexible electrode possible.

During adhesion testing of these specimens, after the initial breakthrough of the top substrate, the crack propagated laterally along the weakest interface. This results in the plateaus observed in the load-displacement curves shown in Figure 3. Prior studies of four point bend testing for adhesion evaluation (Dauskardt et al, 1998;Hughey et al, 2004;Huang et al, 2005) demonstrate horizontal plateaus of brittle systems, whereas the tests performed in this study do not. This may be due to plastic energy absorption from the polyimide, or it may be an effect of loading rate. The effect of loading rate on the load-displacement plateau has been investigated by Hughey et al (2006) and a rate of 0.08μ m/s was advised for equilibrium crack propagation in elastic systems. However, in a polymer-metal system plastic and time dependent deformation effects must be considered. In the current study, a displacement rate of 1.0 μ m/s was used in order to avoid time dependent plastic deformation effects such as creep. This discrepancy between equilibrium crack conditions and the current test conditions may explain the relative non-linearity of the plateau. However, examination of the load-displacement curves in Figure 3 reveals significantly different load plateaus for each system. While the energies shown in the Figure 5 are quantitatively accurate only in the purely elastic case, the relative interfacial strengths are a first order extension for this particular metal-polymer system. Thus, the four point bend test may be used for these polymer-metal systems to determine the relative increase in toughness provided by each adhesion layer. In our study, chromium outperformed tantalum, which outperformed the titanium-tungsten alloy, which was approximately twice as strong an interface as gold deposited upon plasma etched Kapton.

In conclusion, Ti-W was shown to be a suitable adhesion layer for the gold-Kapton system, considering the biocompatibility requirements as well as device durability and demonstrating consistent recording ability over 100 days. The four point bend test was a successful indicator of relative levels of interfacial adhesion energy. We fabricated ECoG electrode arrays which were implanted, and used to record evoked potentials from awake rats. Our measurements

demonstrated that the flexible Kapton substrate-gold ECoG electrode array can detect ERPs from the cortex as efficiently as screw electrodes, but with the potential for high resolution mapping with lower variability and higher fidelity for high frequency components in the evoked responses due to the smaller electrode size and closer tissue proximity. Since most of our animals are still implanted, and being recorded, we do not yet have sufficient post-mortem histological measures, and is the topic of future studies. However, in one animal implanted for 50 days, device failure occurred due to fluid leakage under SU-8, and we did not observe scarring or tissue build-up around the device showing great promise for epidural implants for long term studies. Other adhesion layers that would prove safe for implantation can also be tested in this way to continue to increase device durability and robustness.

Acknowledgements

The authors would like to acknowledge the experimental assistance of Dr. Louis Scudiero at Washington State University with XPS analysis, Dr. T. J. Balk at the University of Kentucky for the Ta/Au film deposition, and Dr. Manuel J. Rojas. The financial support from the W.M. Keck Foundation and the National Institute of Mental Heath under grant numbers MH60263 and MH71830 was greatly appreciated.

References

Bjornsson CS, Oh SJ, Al-Kofahi YA, Lim YJ, Smith KL, Turner JN, De S, Roysam B, Shain W, Kim SJ. Effects of insertion conditions on tissue strain and vascular damage during neuroprosthetic device insertion. J Neural Engineering 2006;3:196–207.

Cheung KC, Renaud P, Tanila H, Djupsund K. Flexible polyimide microelectrode array for in vivo recordings and current source density analysis. Biosensors and Bioelectronics 2007;22:1783–1790. [PubMed: 17027251]

Dauskardt RH, Lane M, Ma Q, Krishna N. Adhesion and debonding of multi-layer thin film structures. Engineering Fracture Mechanics 1998;61:141–162.

Haq KE, Behrndt KH, Kobin I. Adhesion Mechanism of Gold-Underlayer Film Combinations to Oxide Substrates. J. Vac. Sci. Technol. A 1969;6:148–152.

Hetke JF, Najafi K, Wise KD. Flexible Miniature Cables for Long-term Connection to Implantable Sensors. Sensors and Actuators 1990;A21–A23:999–1002.

Hollenberg BA, Richards CD, Richards R, Bahr DF, Rector DM. A MEMS fabricated flexible electrode array for recording surface field potentials. J Neurosci Methods 2006;153(1):147–153. [PubMed: 16352343]

Huang Z, Suo Z, Xu G, He J, Prévost JH, Sukumar N. Initiation and arrest of an interfacial crack in a four-point bend test. Engineering Fracture Mechanics 2005;72:2584–2601.

Hughey MP, Morris DJ, Cook RF, Bozeman SP, Kelly BL, Chakravarty S, Harkens DP, Stearns LC. Four-point bend adhesion measurements of copper and permalloy systems. Engineering Fracture Mechanics 2004;71:245–261.

Jalonen P, Tuominen A. The effect of sputtered interface metallic layers on reinforced core laminate making build-up structures. Microelectronics Reliability 2002;42:1075–1079.

Jones MS, Barth DS. Spatiotemporal organization of fast (>200Hz) electrical oscillations in rat vibrissa/barrel cortex. J Neurophysiol 1999;82(3):1599–1609. [PubMed: 10482773]

Jones MS, MacDonald KD, Choi B, Dudek FE, Barth DS. Intracellular correlates of fast (>200 Hz) electrical oscillations in rat somatosensory cortex. J Neurophysiol 2000;84(3):1505–1518. [PubMed: 10980023]

Kim S, Zoschke K, Klein M, Black D, Buschick K, Toepper M, Tathireddy P, Harrison R, Oppermann H, Solzbacher F. Switchable polymer-based thin film coils as a power module for wireless neural interfaces. Sensors and Actuators A: Physical 2007;136(1):467–474.

Lawrence SM, Dhillon GS, Horch KW. Fabrication and characteristics of an implantable, polymer-based, intrafascicular electrode. J Neurosci Methods 2003;131:9–26. [PubMed: 14659819]

Mailley S, Hyland M, Mailley P, McLaughlin JA, McAdams ET. Thin film platinum cuff electrodes for neurostimulation: in vitro approach of safe neurostimulation parameters. Bioelectrochemistry 2004;63:359–364. [PubMed: 15110303]

Matsuno H, Yokoyama A, Watari F, Uo M, Kawasaki T. Biocompatability and osteogenesis of refractory metal implants, titanium, hafnium, niobium, tantalum and rhenium. Biomaterials 2001;22:1253–1262. [PubMed: 11336297]

Maynard EM, Fernandez E, Normann RA. A technique to prevent dural adhesions to chronically implanted microelectrode arrays. J Neurosci Methods 2000;97:93–101. [PubMed: 10788663]

Merrill DR, Bikson M, Jefferys JGR. Electrical stimulation of excitable tissue: design of efficacious and safe protocols. J Neurosci Methods 2005;141:171–198. [PubMed: 15661300]

Nakamura Y, Suzuki Y, Watanabe Y. Effect of oxygen plasma etching on adhesion between polyimide films and metal. Thin Solid Films 1996;290–291:367–369.

Penfield W, Boldrey E. Somatic motor and sensory representation in the cerebral cortex of man as studied by electrical stimulation. Brain 1937;60:389–443.

Polikov VS, Tresco PA, Reichert WM. Response of brain tissue to chronically implanted neural electrode. J Neurosci Methods 2005;148:1–18. [PubMed: 16198003]

Pommersheim J, Nguyen T, Zhang Z, Lin C. Cation Diffusion at the Polymer Coating / Metal Interface. J. Adhesion Sci. Tech 1995;9(7):935–951.

Prigg T, Goldreich D, Carvell GE, Simons DJ. Texture discrimination and unit recordings in the rat whisker/barrel system. Physiology and Behavior 2002;77:671–675. [PubMed: 12527017]

Rector DM, George JS. Continuous image and electrophysiological recording with real time processing and control. Methods 2001;25(2):151–163. [PubMed: 11812203]

Schmidt S, Horch K, Normann R. Biocompatibility of silicon-based electrode arrays implanted in feline cortical tissue. J Biomed Mater Res 1993;27(11):1393–1399. [PubMed: 8263001]

Soden D, Morrissey A, Collins C, Piggott J, Larkin J, Norman A, Aarons S, Dunne C, O'Sullivan GC. Electrotherapy of tumour cells using flexible electrode arrays. Sensors and Actuators B 2004;103:219–224.

Stieglitz T, Meyer JU. Implantable Microsystems: Polyimide-Based Neuroprostheses for Interfacing Nerves. Medical Device Technology 1999;10(6):28–30. [PubMed: 10623349]

Stieglitz T, Ruf HH, Gross M, Schuettler M, Meyer JU. A biohybrid system to interface peripheral nerves after traumatic lesions: design of a high channel sieve electrode. Biosensors and Bioelectronics 2002;17:685–696. [PubMed: 12052354]

Strumwasser F. Long-Term Recording from Single Neurons in Brain of Unrestrained Mammals. Science 1958;127(3296):469–470. [PubMed: 13529005]

Supriya L, Claus RO. Solution-Based Assembly of Conductive Gold Film on Flexible Polymer Substrates. Langmuir 2004;20:8870–8876. [PubMed: 15379520]

Szarowski DH, Andersen MD, Retterer S, Spence AJ, Isaacson M, Craighead HG, Turner JN, Shain W. Brain responses to micro-machined silicon devices. Brain Research 2003;983:23–35. [PubMed: 12914963]

Woolsey TA, Van der Loos H. The structural organization of layer IV in the somatosensory region (SI) of mouse cerebral cortex. Brain Res 1970;17:205–242. [PubMed: 4904874]

Yeager JD, Bahr DF, Rector DM, Richards CD, Richards RF. Design and development of metal - polymer film systems for flexible electrodes used in cortical mapping. ASM MPMD Proceedings. 2007In Press

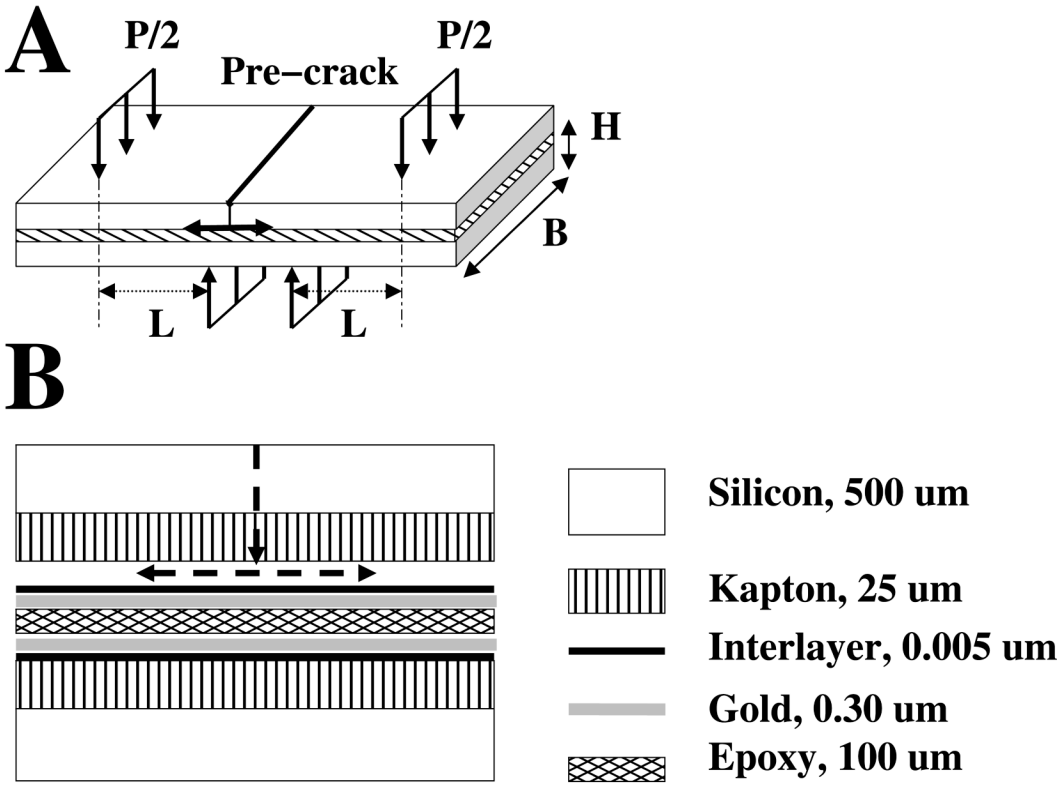

Figure 1.

Panel (A) illustrates a schematic of a four point bend test with relevant dimensions labeled. The crack starts at the pre-crack initiation site, travels down through the sample, and moves laterally along the interface of interest. The distance *L* is measured between an inner and outer pins (three vertical arrows), *P* is the applied load, and *B* and *H* are respectively the width and height of the specimen. Panel (B) shows a cross section of sandwich specimen electrode array for four point bend test. The layers are not to scale in order to show detail, and the desired crack path is shown with the arrows.

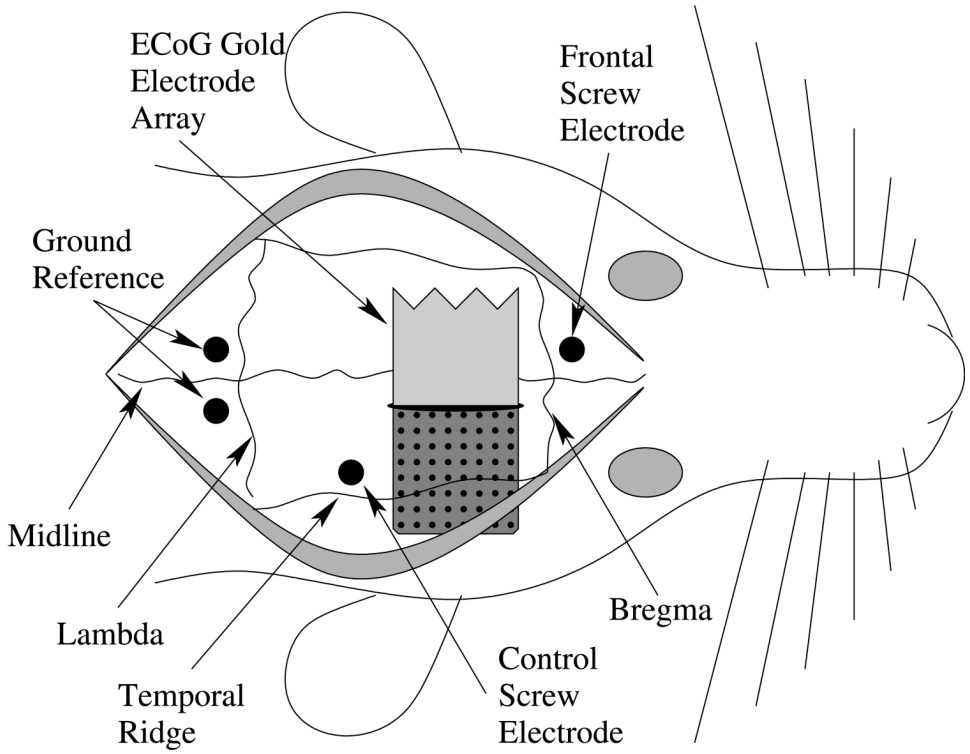

Figure 2.
Depiction of the implanted electrode location within the rat. The 64 channel ECoG electrode array was 5×5 mm in size, inserted through a slot cut into the bone, 1mm lateral to Midline, and 1mm caudal to Bregma. Stainless steel screws were placed over the frontal lobe to determine the animal behavioral state, next to the electrode array to serve as a control screw electrode, and two screws placed over the occipital lobe served as ground reference electrodes.

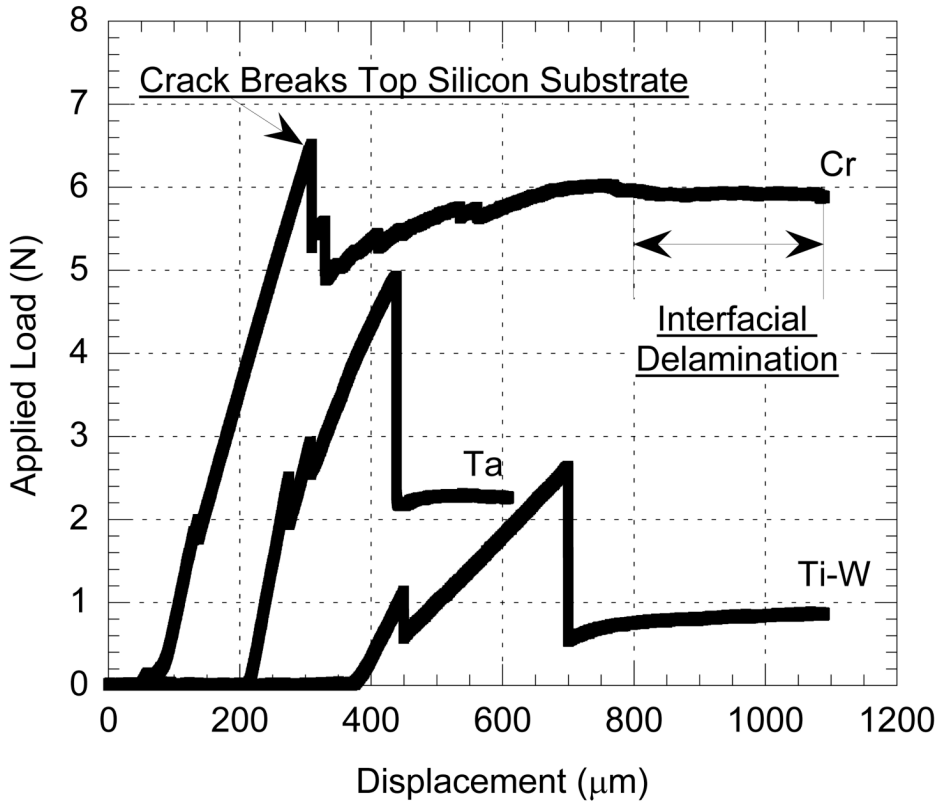

Figure 3.
Typical load-displacement curves for chromium (Cr), tantalum (Ta), and titanium-tungsten (Ti-W) adhesion layer samples. Curves have been offset in displacement by 200 um on the x-axis for clarity. The peak of each curve shows the load required to break the top substrate. The strongest adhesion layer is Cr, followed by Ta and Ti-W.

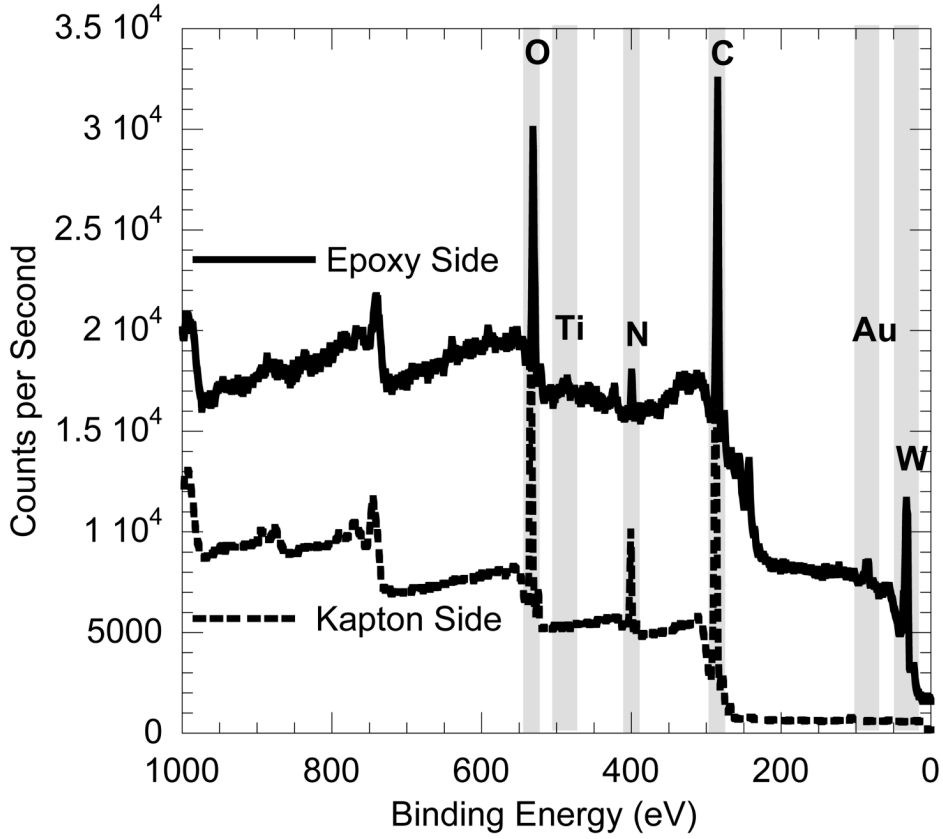

Figure 4.
XPS spectra of a Ti-W adhesion layer sample after delamination, showing that the Titanium (Ti), Tungsten (W) and Gold (Au) layers delaminate from the Kapton. The Nitrogen (N), Oxygen (O), and Carbon (C) peaks are typical atmospheric contaminants as well as constituent chemistry of the Kapton film.

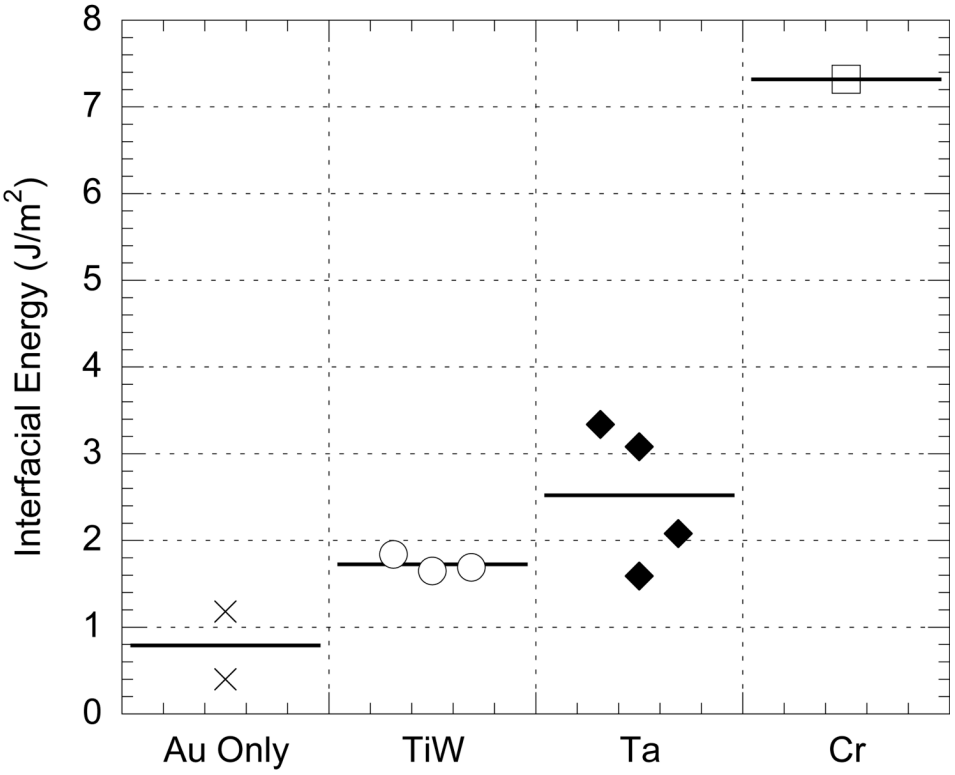

Figure 5.
Four point bend test results for Gold-Kapton with gold alone and three adhesion layers show each measured value for interfacial energy and the average for each layer denoted by a horizontal bar.

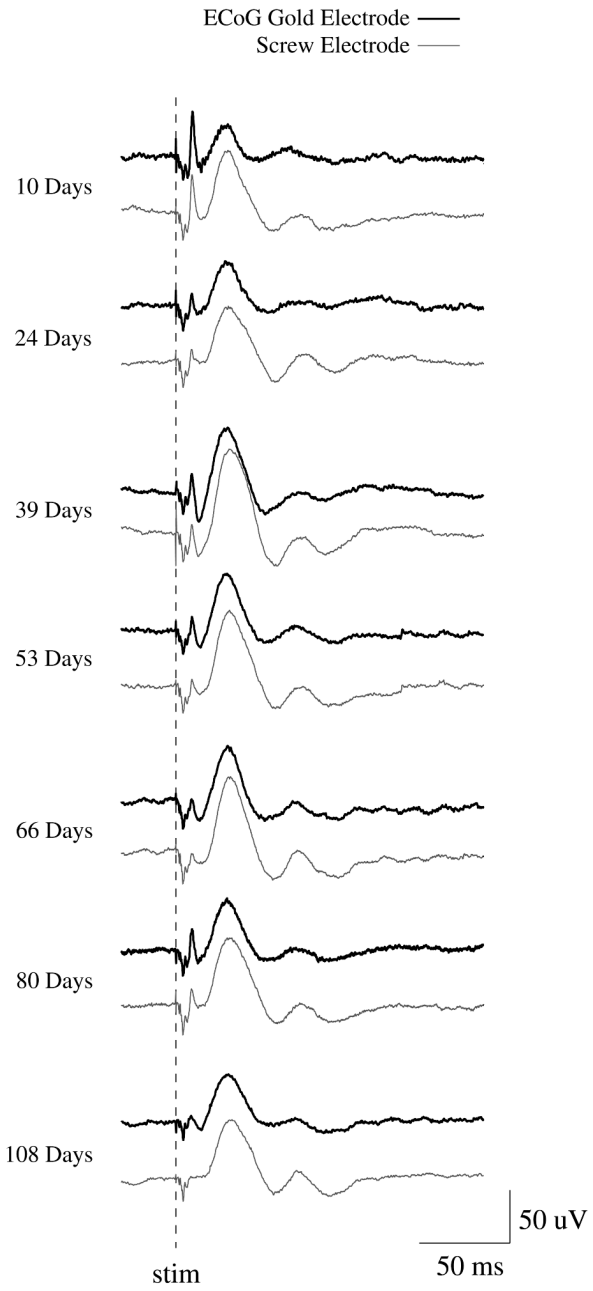

Figure 6.
Average surface evoked responses from a typical implanted animal shows a qualitative assessment of signals from the ECoG and screw electrodes across time. We found consistent electrical signals during external stimulation in both the ECoG gold electrode array and the control screw electrode at 10 to 108 days post implantation.

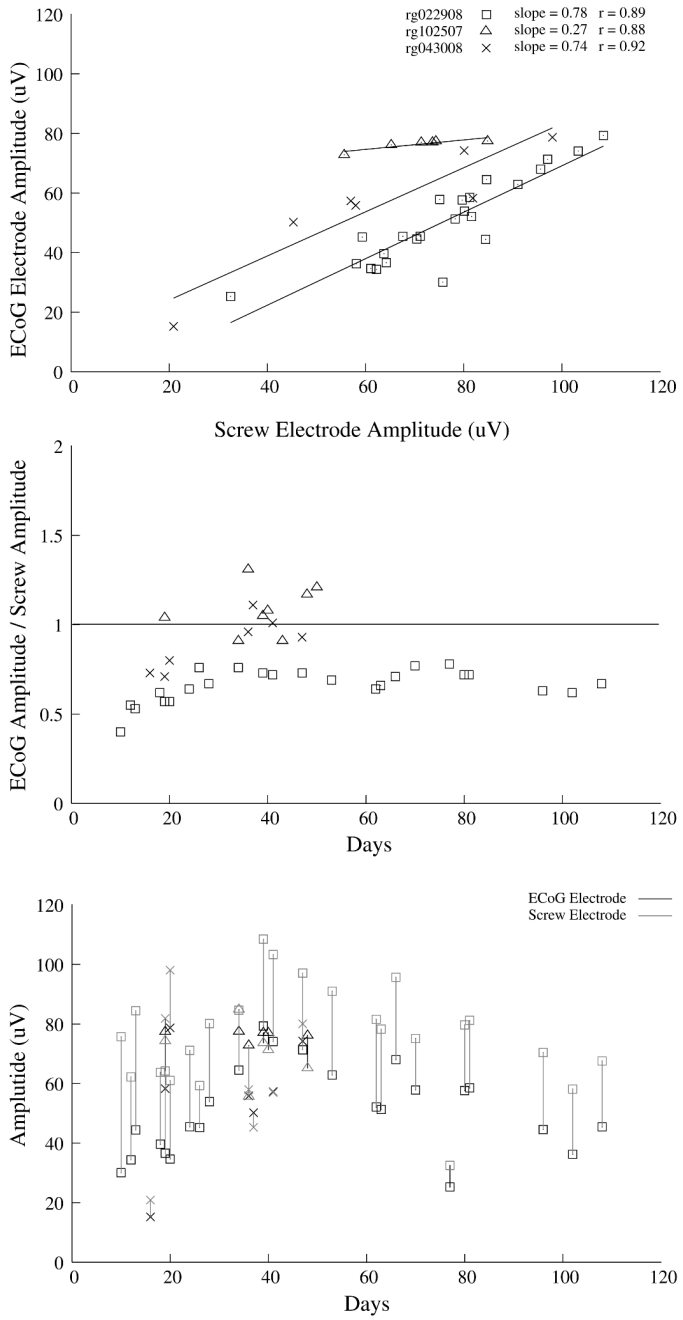

Figure 7.

The average amplitude for the surface evoked responses across time shows consistent values for both the ECoG gold electrode array (black symbols) and the screw electrode (gray symbols, lower panel). The vertical bars in the lower panel are used to match ECoG and screw electrode values from the same recording period. Since it was difficult to present the same stimulus amplitude across days, there is much day-to-day variability in the lower panel, thus we compared the relative amplitude of the ECoG and screw eletcrode signals by plotting their ratio across recording day (middle panel). When plotting the the amplitude of the ECoG electrode as a function of the screw electrode amplitude (top panel), we find a good correlation (r~0.9) with slopes less than one, indicating that the screw electrode amplitudes were consistently

higher than the ECoG amplitudes. The three different shaped symbols indicate data from three animals.

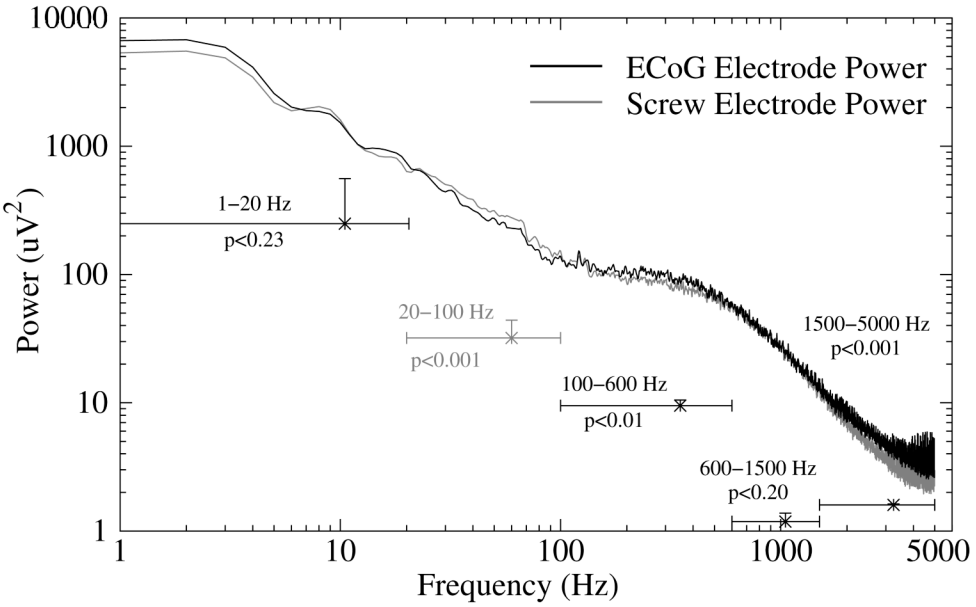

Figure 8.

The evoked response frequency components recorded by the ECoG and screw electrodes were calculated using a Fast Fourier Transform, then the power of each frequency was averaged across all animals and plotted (black=ECoG, gray=Screw Electrodes). The frequency power data was then averaged into bins from 1–20Hz, 20–100Hz, 100–600Hz, 600–1500Hz and 1500–5000Hz, and the mean power difference between the ECoG electrode and screw electrode was plotted on the same axis (horizontal bars). A paired t-test comparison for each bin revealed significant differences in the frequency components such that the screw electrode power was significantly higher than the ECoG electrode power between 20 and 100 Hz ($p<0.001$), and the ECoG electrode power was higher for frequencies greater than 100 Hz.